Synthesis of Polypyrrole Nanoparticles in Natural Rubber–Polystyrene Blend via Emulsion Polymerization

Hassan Ghalib, Ibrahim Abdullah, Rusli Daik

School of Chemical Sciences and Food Technology, Faculty of Science and Technology, Universiti Kebangsaan Malaysia, 43600 UKM Bangi, Selangor, Malaysia

Received 21 July 2010; accepted 19 April 2011
DOI 10.1002/app.34714
Published online 23 August 2011 in Wiley Online Library (wileyonlinelibrary.com).

ABSTRACT: Nanoparticles of polypyrrole (PPy) in 40/60 wt % natural rubber (NR)–polystyrene (PS) blends were synthesized by emulsion polymerization using ferric sulfate [Fe_2 $(SO_4)_3$], sodium dodecyl sulfate (SDS), and *n*-amyl alcohol as the oxidant, surfactant, and cosurfactant, respectively. The NR/PS/PPy blends were characterized by Fourier transform infrared spectroscopy (FTIR), elemental analysis, thermogravimetric analysis (TGA), and field emission scanning electron microscopy (FESEM). FESEM micrographs showed that NR/PS/PPy blends were homogeneous, and PPy nanoparticles were well distributed throughout the binary matrix of NR/PS. The size of PPy particles in the blends was in the range of 26–80 nm. The electrical conductivities of the pellets prepared from NR/PS/PPy blends increased as the composition of PPy nanoparticles was increased, which were in the range of 8.9×10^{-8} – 2.89×10^{-4} S/cm. Thermal stability of the blends increased as the content of PPy was increased, as shown by TGA thermograms. © 2011 Wiley Periodicals, Inc. J Appl Polym Sci 123: 2115–2121, 2012

Key words: natural rubber; emulsion polymerization; conducting polymers; nanocomposites; polypyrroles

INTRODUCTION

In the recent years, blending of two or more polymers to create new polymeric materials, which possess a combination of unique properties, has attracted a great deal of attention as novel materials. Blending of insulating polymers with conducting polymers produces a new polymeric material with unique mechanical and electrical properties.[1] PPy is one of the few conducting polymers, which has relatively high electrical conductivity, easy to synthesis, and good environmental stability. However, brittleness and lack of processability limit their extensive applications.[2]

Natural rubber (NR) is a solid material, which is characterized by good elastic property, good resilience, and damping behavior but poor chemical resistance and processability.[3,4] Meanwhile, polystyrene (PS), a thermoplastic polymer exhibits superior processing characteristics, but it is extremely brittle.[5] NR and PS are insulating polymers, whereas PPy is a conducting polymer; therefore, a blend of them is expected to exhibit electrical conductivity, good flexibility, impact strength, and processability. PPy blends can be prepared by either chemical[6,7] or electrochemical oxidation.[8] There were several synthetic routes reported for the preparation of PPy blend: chemicals *in situ* polymerization,[9] emulsion polymerization,[10] and dispersion polymerization.[11]

Emulsions are thermodynamically unstable liquid/liquid dispersions that are stabilized, in general, by surfactants.[12] The key role of a surfactant is to participate in the nucleation step and contribute to the creation of stable droplets. The final number of droplets is directly related to the initial concentration of the surfactant. Another role of the surfactant is to impart good stability to the droplets during polymerization as well as storage.[13] Many studies have reported the preparation of conducting polymer in an insulating polymer matrix. Kim and Kim[10] prepared polypyrrole–polycaprolactone blend by emulsion polymerization using dodecylbenzene sulfonic acid as the emulsifier and dopant. Sun and Ruckenstein[14] prepared (styrene–butadiene–styrene) triblock rubber composites by means of forming an inverted emulsion through dispersing aqueous $FeCl_3$ in an organic solution of rubber and a nonionic surfactant. This is followed by adding pyrrole solution dropwise to form PPy composite.

Omastova et al.[15] reported the formation of PPy composites with polyethylene, polypropylene, and poly(methylmethacrylate) by a chemical polymerization method, resulting in a network-like structure of PPy embedded in the insulating polymer matrix. Xie et al.[16] synthesized PPy composites by *in situ* polymerization using $FeCl_3$ as the oxidant in the presence of chlorinated polyethylene powder (CPE) suspension and NR latex, respectively. According to their work, the PPy/CPE and PPy/NR composites showed

Correspondence to: R. Daik (rusli@ukm.my).

a percolation threshold of conductivity at about 12% and 6%, respectively. With the increase of PPy content, the tensile strength of both types of composites increased while the ultimate elongation decreased, but that the tensile strength of the PPy/NR composites decreased at PPy content higher than 50%. Synthesis of PPy ultrathin films on NR latex particles (core-shell structure) via admicellar polymerization was also reported.[17] The presence of salt, the surfactant adsorption, and pyrrole adsolubilization was enhanced, which resulted in a smooth and homogeneous coating of PPy onto the latex surface, and a higher electrical conductivity (1.45×10^{-6} S cm^{-1}) than PPy-coated latex prepared without salt (0.96×10^{-6} S cm^{-1}). However, the electrical conductivity of PPy-coated latex prepared with/without salt showed a big improvement compared with that of pure NR (10×10^{-15} S cm^{-1}). Lascelles and Armes[18] studied the synthesis of PPy-coated micrometer-sized poly(*N*-vinylpyrrolidone)-stabilized PS latices by way of the *in situ* polymerization of a conducting polymer from aqueous solution. The resulting composites exhibited conductivities similar to those of PPy bulk powder (2–6 S cm^{-1}) even at PPy loadings as low as 6 wt %. Xiao-Jun et al.[19] synthesized nanosized PPy-PS composite particles by polymerization of pyrrole on PS nanoparticles in the presence of $FeCl_3$ as oxidant and stabilized by a cationic nonpolymerizable surfactant cetyltrimethylammonium bromide (CTAB), a nonionic polymerizable surfactant ω-methoxy[poly-(ethylene oxide)$_{40}$]undecyl α-methacrylate (PEO-*R*-MA-40), or a cationic polymerizable surfactant ω-acryloyloxyundecyltrimethyl-ammonium bromide (AUTMAB). It was found that, when a cationic nonpolymerizable surfactant (CTAB) was used as stabilizer the electrical conductivities were between ($\sim 10^{-7}$ and 10^{-3} S cm^{-1}); however, when a nonionic polymerizable surfactant (PEO-*R*-MA-40) or a cationic polymerizable surfactant (AUTMAB) was used, the electrical conductivities were $\sim 10^{-5} - 10^{-1}$ S cm^{-1}.

This work reports the preparation of PPy nanoparticles in NR–PS blend at a weight ratio of 40/60 by emulsion polymerization using ferric sulfate [$Fe_2(SO_4)_3$], sodium dodecyl sulfate (SDS), *n*-amyl alcohol as oxidant, surfactant, and as cosurfactant, respectively. The morphological, electrical conductivity, and thermal properties of the NR/PS/PPy blends were described.

EXPERIMENTAL

Materials

NR (SMR-L) was supplied by Rubber Research Institute of Malaysia and PS by Idemitsu Petrochemicals (M) Sdn. Bhd. SDS and aluminum oxide were purchased from Merck, and pyrrole of 97% purity from Aldrich was purified by passing through a column of activated basic alumina and stored at 4°C before use. The oxidant, ferric sulfate $Fe_2(SO_4)_3$ was purchased from Riedel-De Haen Ag Seelze-Hannover, *n*-amyl alcohol from BDH chemicals Ltd Poole England, and Toluene of 99.5% purity from Systerm. All chemicals were used as received without purification. Deionized water was used in all experiments.

TABLE I
Pyrrole Monomer and $Fe_2(SO_4)_3$ Used for the Preparation of NR/PS/PPy Blends

Samples	NR/PS (wt %)	Py (mL)	$Fe_2(SO_4)_3$ (g)
NR/PS/PPy	40/60	2	11.6
NR/PS/PPy	40/60	3	17.2
NR/PS/PPy	40/60	4	23.2
NR/PS/PPy	40/60	6	34.4

Preparation of the NR/PS/PPy blends

Blends of NR/PS at a weight ratio of 40/60 with PPy were prepared by emulsion polymerization at room temperature. In a typical experiment, 3.6 g NR and 6.24 g PS (host polymer) were soaked in 200 mL toluene in a flask and mechanically stirred. A solution of an appropriate amount of pyrrole monomer and 4 mL of *n*-amyl alcohol in 30 mL toluene were added dropwise to the mixture. After 3 h, an aqueous solution of 20 g SDS in 100 mL deionized water was introduced into the flask; thus, an emulsion was generated. The stirring was continued for 3 h. Then, a solution of an appropriate amount of $Fe_2(SO_4)_3$ in 50 mL of deionized water was introduced dropwise into the emulsion under constant stirring (300 rpm). Polymerization was allowed to proceed for 5 h. The NR/PS/PPy emulsion was precipitated by pouring into methanol. The precipitate was filtered and washed several times with methanol and deionized water until the washing became colorless. The blend recovered was dried in an oven at 50°C for 48 h. The amount of $Fe_2(SO_4)_3$ and pyrrole monomer added to 40/60 NR/PS blends was given as presented in Table I.

Characterization

The Fourier transform infrared spectroscopy (FTIR) spectra of the blends were obtained via KBr pellets on a Perkin–Elmer FTIR system Spectrum GX. The spectra were recorded over a frequency range of 600–4000 cm^{-1}.

The composition of PPy in the blend was determined via elemental analysis using a CHNS/Thermo Finnigan/Eager 300 for EA 1112 elemental analyzer.

The specimens used for conductivity measurement were in pellet form with a diameter and thickness of

13 mm and 1.5 mm, respectively. The pressure used to compress the samples was 5 ton, and the whole process took around 5 min. Samples obtained were analyzed by using frequency response analyzer (Solatron Schlumberger 1260 HF). Impedance spectrum was recoded over a frequency range of 1 Hz–10 MHz at room temperature.

Field emission scanning electron microscopy (FESEM) images were recorded with a SUPRA 55VP microscope (Zeiss, Germany). The hot-pressed samples were fractured in liquid nitrogen, and the broken surface was subjected to observation.

Thermal stability was studied by using thermogravimetry analyzer TGA/Sdta851 (Mettler-Toledo).

RESULTS AND DISCUSSION

Elemental analysis

By using the calculated percentage of nitrogen from elemental analysis of the blends, the content of PPy in the blends was estimated. The content of PPy (C_{PPy}) in blends was determined from the calculated theoretical mass of nitrogen in blends and the nitrogen content from elemental analysis. The theoretical mass of nitrogen in blends[3] and amount of PPy (C_{PPy}) in blends are calculated as follows:

$$C_T = \frac{M_N}{M_{Py}} \times 100, \quad (1)$$

$$C_{PPy} = \frac{C_N}{C_T} \times 100, \quad (2)$$

where C_T, M_N, M_{Py}, and C_N are the theoretical mass of nitrogen in blends, molecular mass of nitrogen, molecular weight of Py unit, and content of nitrogen calculated from elemental analysis, respectively.

Results of elemental analysis, nitrogen content, and PPy content in blends are shown in Table II.

FTIR spectroscopy

The Fourier transform infrared spectroscopy (FTIR) spectra of PPy, 40/60 NR/PS blend, and NR/PS/PPy blends containing 8.6, 11.0, 21.1, and 27.3 wt % PPy, respectively, are shown in Figure 1. The bands at 1542 cm^{-1} (the asymmetric and symmetric C=C/C—C stretching), 1450 cm^{-1} (C—N stretching), 1269 cm^{-1} (C—N in-plane deformation), and 1052 cm^{-1}

TABLE II
The Amount of PPy as Calculated from the Elemental Analysis of PPy/NR/PS Blends

Samples	Amount of Py monomer (mL)	N (%)	C (%)	H (%)	S (%)	PPy (wt %)
NR/PS/PPy	2	1.39	67.99	7.23	0.70	8.6
NR/PS/PPy	3	1.58	59.44	6.02	0.87	11.0
NR/PS/PPy	4	4.21	81.91	8.33	0.45	21.1
NR/PS/PPy	6	5.13	75.55	7.92	1.34	27.3

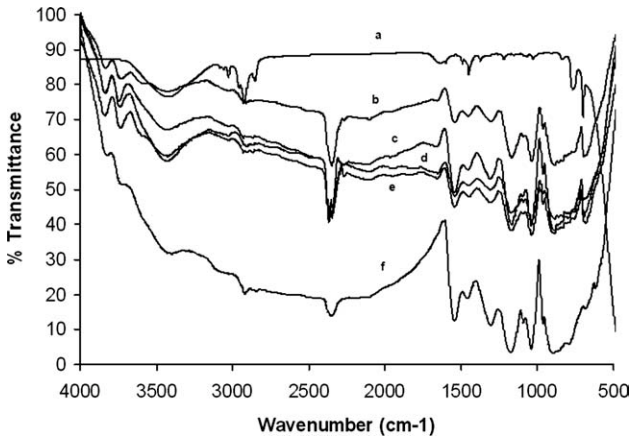

Figure 1 FTIR spectra of (a) 40/60 NR/PS blend, NR/PS/PPy blends containing (b) 8.6 wt % PPy, (c) 11.0 wt % PPy, (d) 21.1 wt % PPy NR, (e) 27.3 wt % PPy, and (f) PPy.

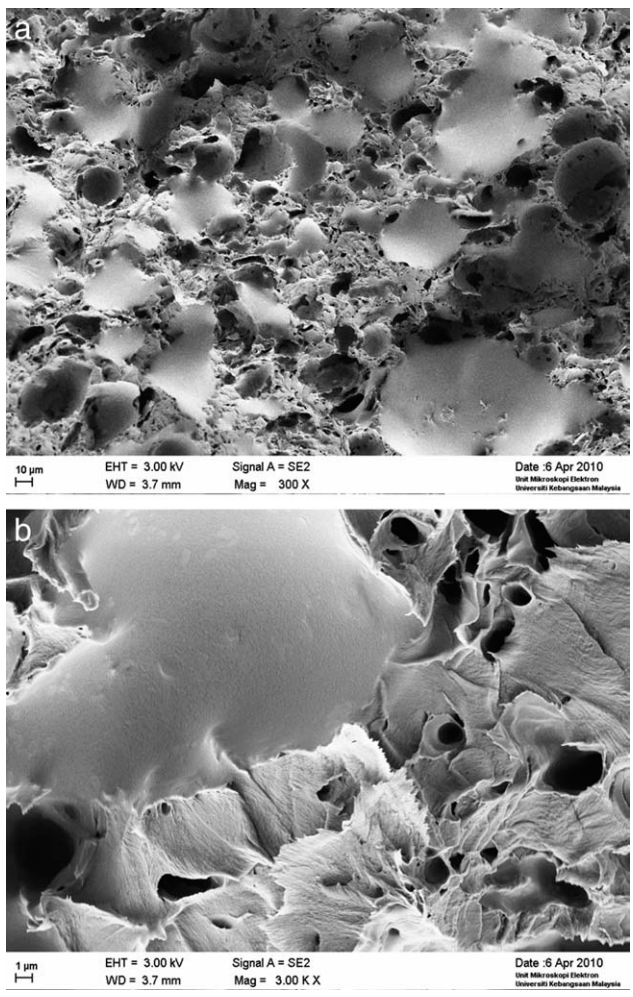

Figure 2 FESEM images of the 40/60 NR/PS blend at different magnification: (a) ×300 and (b) ×3000.

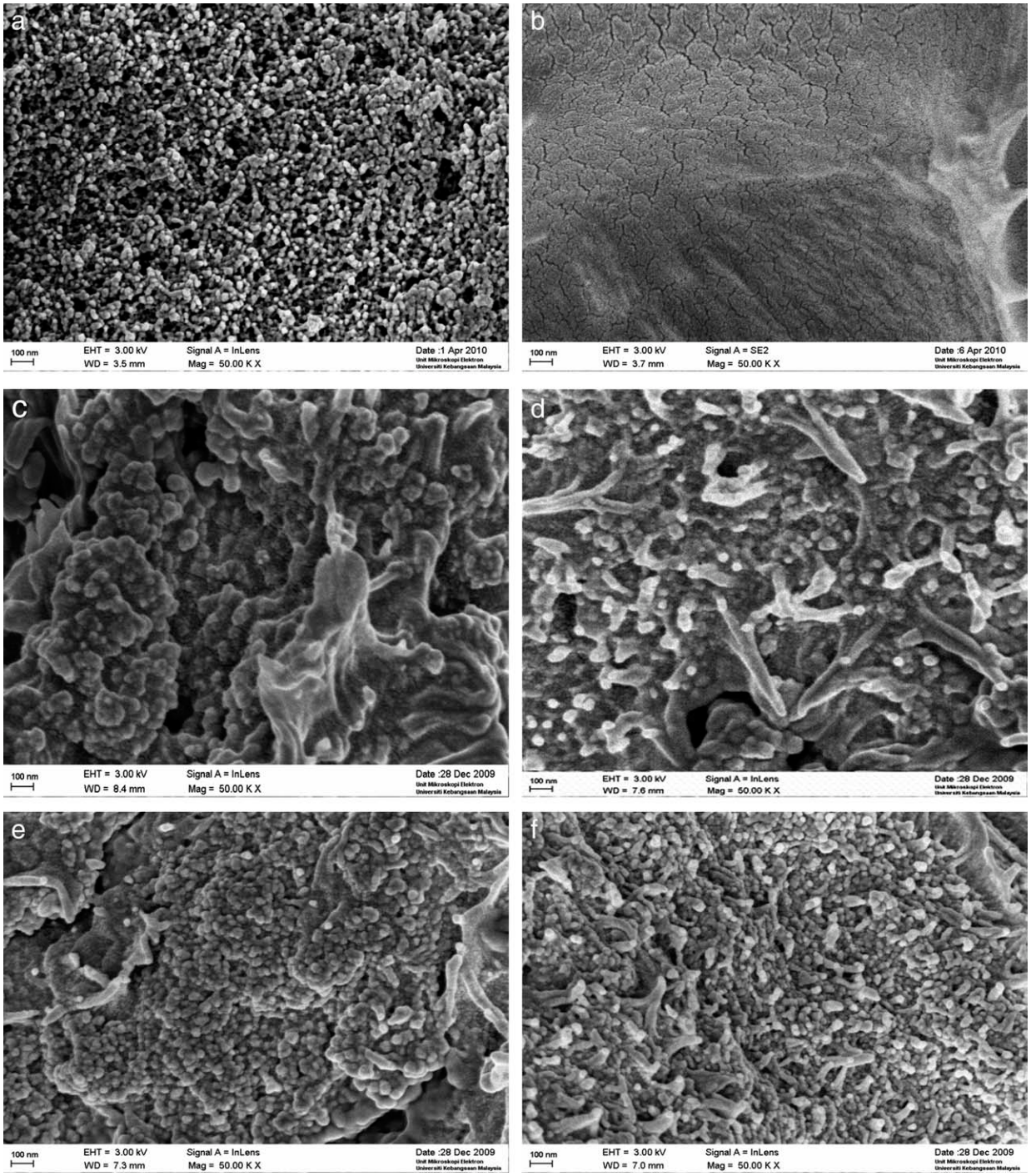

Figure 3 FESEM images of (a) PPy, (b) 40/60 NR/PS blend, NR/PS/PPy blends containing (c) 8.6 wt % PPy, (d) 11.0 wt % PPy, (e) 21.1 wt % PPy NR, and (f) 27.3 wt % PPy.

(C—H in-plane deformation vibration) are the characteristic peaks of PPy. All these peaks are consistent with previous reports.[20,21] The FTIR spectrum of 40/60 NR/PS blend shows those characteristic peaks of PS and NR. The aliphatic and aromatic C—H stretching peaks are in the range of 3028–2855 cm^{-1}. The aliphatic C=C stretching peak is at 1642 cm^{-1}, whereas the aromatic C=C stretching peak is in the range of 1601–1452 cm^{-1}. The FTIR spectra of

TABLE III
Electrical Conductivity of NR/PS/PPy Blends

Blends	Conductivity (S cm^{-1})
NR/PS/PPy, 40/60/8.6 wt %	8.9×10^{-8}
NR/PS/PPy, 40/60/11.0 wt %	2.0×10^{-7}
NR/PS/PPy, 40/60/21.1 wt %	2.1×10^{-6}
NR/PS/PPy, 40/60/27.3 wt %	2.89×10^{-4}

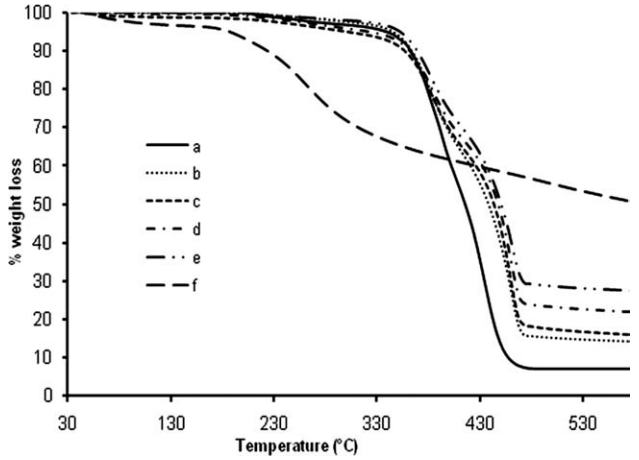

Figure 4 TGA thermograms of (a) 40/60 NR/PS blend, NR/PS/PPy blends containing (b) 8.6 wt % PPy, (c) 11.0 wt % PPy, (d) 21.1 wt % PPy NR, (e) 27.3 wt % PPy, and (f) PPy.

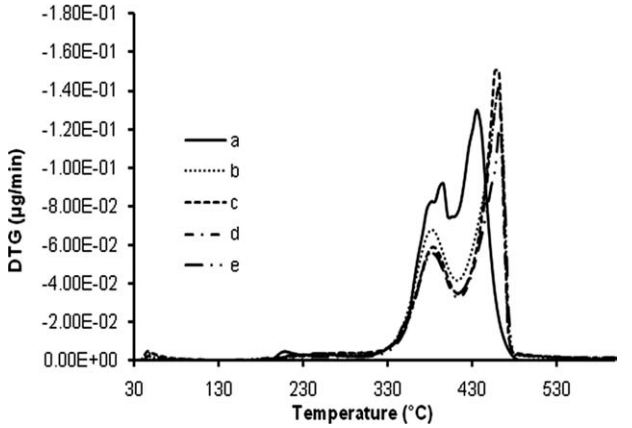

Figure 5 DTG thermograms of (a) 40/60 NR/PS blend, NR/PS/PPy blends containing (b) 8.6 wt % PPy, (c) 11.0 wt % PPy, (d) 21.1 wt % PPy NR, and (e) 27.3 wt % PPy.

NR/PS/PPy blends show absorptions that confirm the incorporation of PPy in the 40/60 NR/PS blend.

The morphology

Previous works indicated that NR/PS blends are incompatible and immiscible.[22–24] To improve the compatibility and homogeneity of blends, various techniques were used. In this study, the homogeneity of NR/PS blend was found to be improved by using emulsion-blending technique. Figure 2 shows FESEM images of the 40/60 NR/PS blends at different magnification. The components with high volume fraction have tendency to become continuous phase relative to that of other components[25]; therefore, in this case, NR will form the dispersed phase, while PS the continuous phase. The NR domain size in the NR/PS blend prepared by emulsion-blending technique was found to be smaller when compared with that of the NR/PS blends prepared by either melt blending or solution blending, as reported by other researchers.[25]

Figure 3 shows FESEM micrographs of PPy and NR/PS/PPy blends containing 0, 8.6, 11.0, 21.1, and 27.3 wt % PPy, respectively. It is apparent that spherical nanoparticles of PPy are well distributed throughout the 40/60 wt % NR/PS blend with particle size of about 26–80 nm. For the case of PPy nanoparticles prepared under the same conditions but without host polymer, one can identify spherical nanoparticles with the size in the range of 30–50 nm [Fig. 3(a)]. In the NR/PS/PPy blend containing 8.6 [Fig. 3(c)] and 11.0 wt % PPy [Fig. 3(d)], PPy nanoparticles are dispensed in matrix and located quite a part from each other, while in the NR/PS/PPy blend-containing 21.1 wt % PPy [Fig. 3(e)], the image shows a homogenous blend with even smaller PPy particles. It can also be seen that the PPy nanoparticles are closely packed. Meanwhile, the image for NR/PS/PPy blend containing 27.3 wt % PPy [Fig. 3(f)] shows that some PPy nanoparticles formed rodlike shape,[26] together with the spherical shape nanoparticles. When the amount of Py monomer increased, more PPy nanoparticles formed in the blend, and these particles gradually grow into the longitudinal direction to form rodlike shape particles.[20,27]

Electrical conductivity

The electrical conductivity of the cold-pressed NR/PS/PPy blends was listed in Table III. The electrical conductivity of the blends increases with increasing amount of PPy in the blends, from 8.9×10^{-8} to

TABLE IV
Summary of the Decomposition Processes for NR/PS and NR/PS/PPy Blends

Blends	Initial degradation temperature (°C)	% Weight loss (°C)			Residue at 600°C (%)
		200–350	350–410	410–470	
NR/PS, 40/60	355	6.81	32.92	52.36	7.17
NR/PS/PPy, 40/60/8.60 wt %	354	5.79	30.29	47.98	14.01
NR/PS/PPy, 40/60/11.01 wt %	355	8.63	26.24	46.77	15.50
NR/PS/PPy, 40/60/21.10 wt %	360	7.65	25.14	43.19	21.47
NR/PS/PPy, 40/60/27.31 wt %	366	4.72	24.95	40.63	27.41

2.89×10^{-4} S cm^{-1}. NR and PS are insulating materials with NR having an electrical conductivity of 7.18×10^{-15} S cm^{-1}[28] and PS of 1×10^{-16} S cm^{-1}. In this study, the insulating NR/PS blend showed an electrical conductivity of 8.1×10^{-16} S cm^{-1}. The NR/PS/PPy blends, containing 8.6 and 11.0 wt % PPy, show electrical conductivity of 8.9×10^{-8} and 2.0×10^{-7} S cm^{-1}, respectively. The low values of conductivity found for these two samples may be due to the PPy nanoparticles that are located quite away from each other as shown in Figure 3(c,d). This caused difficulties in interparticle electron hopping resulting in smaller conductivity. The NR/PS/PPy blend that contains 21.1 wt % PPy showed an electrical conductivity of 2.1×10^{-6} S cm^{-1}. As shown in Figure 3(e), the PPy nanoparticles are closely packed and thus facilitating the interparticle electron hopping and resulting in relatively high conductivities. The highest electrical conductivity found was 2.89×10^{-4} S cm^{-1}, as exhibited by the NR/PS/PPy blend containing 27.3 wt % PPy, which is about 12 orders of magnitude higher than that of 40/60 NR/PS blend. As mentioned earlier, the NR/PS/PPy blend that contains 27.3 wt % of PPy [Fig. 3(f)] showed that some PPy formed rod-like shape particles. It was reported that PPy nanorods had the main-chain structure identical to granular PPy, and their conductivity and thermal stability were superior to that of granular PPy.[26]

Thermal stability study

The TGA thermograms for PPy nanoparticales, 40/60 NR/PS blend and NR/PS/PPy blends containing 8.60, 11.01, 21.10, and 27.31 wt % PPy are shown in Figure 4, while Figure 5 presents the DTG thermograms of respective blends. Table IV presents the summary of the decomposition steps of all samples. It can be seen from the TGA curves that the PPy nanoparticles reveal two stages of mass loss. The initial mass loss, below 100°C, is attributed to the release of adsorbed moisture in the PPy. The second mass loss, starting around 189°C and continues to 600°C can be attributed to decomposition of SDS residue and also to gradual decomposition of the PPy chains. The 49.70% residue of PPy at 600°C points out that PPy is quite thermally stable as also reported by other researchers.[29,30] In the case of NR/PS blend, a three-step weight loss is clearly observed. The first mass loss (6.81 wt %), ranging from 200 to 350°C, can be attributed to the loss of SDS residue and early decomposition of NR. The second weight loss (32.92 wt %), ranging from 350 to 410°C, attributed to the decomposition of the NR.[28] The third mass loss (52.36 wt %), ranging from 410 to 470°C, attributed to the decomposition of the PS.[31] It is obvious that all NR/PS/PPy blends show the same decomposition patterns to that of the NR/PS blend with improved thermal stability in three steps of mass loss. The first one, around 180–350°C is due to the decomposition of SDS,[21] and early decomposition of PPy, the second at 350–410°C resulted from the decomposition of the NR,[28] and the third at 410–470°C resulted from the decomposition of the PS.[31] One can see that as the PPy content is increased, the value of the initial decomposition temperature (°C) of the NR/PS/PPy blends is increased accordingly, together with a decrease in the mass loss of the blends. PPy is known for its relatively high thermal stability compared to other polymers.[29,30] Therefore, the incorporation PPy exerts a stabilizing effect on the blends[28,32]

CONCLUSIONS

NR/PS/PPy conductive blends have successfully been prepared by the emulsion polymerization of an organic solution of Py dispersed in the emulsion of 40/60 NR/PS as the continuous phase. The incorporation of PPy into the NR/PS matrix was confirmed by FTIR spectroscopy. The use of emulsion-dispersion technique has enabled the formation of homogeneous blends of NR and PS. The formation of PPy nanoparticles within the NR/PS matrix was observed by FESEM with the size range of 26–80 nm. The conductivity of the blends increased with the increasing content of PPy, which were in the range of 8.9×10^{-8} – 2.89×10^{-4} S cm^{-1}. The thermal stability of the NR/PS blend was also enhanced upon blending with PPy.

References

1. Yang, J.; Yang, Y.; Hou, J.; Zhang, X.; Xu, W. Z. M. Polymer 1996, 37, 793.
2. Wang, L.-X.; Li, X.-G.; Yang, Y.-L. React Funct Polym 2001, 47, 125.
3. Hosseini, S. H.; Ali, A. E. J Appl Polym Sci 2003, 90, 49.
4. Ibrahim, A.; Dahlan, M. Prog Polym Sci 1998, 23, 665.
5. Park, B. J.; Kim, T. H.; Choi, H. J.; Lee, J. H. J Macromol Sci B: Phys 2007, 46, 341.
6. Abraham, D.; Jyotsna, T. S.; Subramanyam, S. V. J Appl Polym Sci 2001, 81, 1544.
7. Zoppi, R. A.; Paoli, M.-A. D. Polymer 1999, 37, 1996.
8. Aguilar-Hernàndez, J.; Potje-Kamlot, K. J Phys D: Appl Phys 2001, 34, 1700.
9. Jesus, M. C. D.; Fu, Y.; Weiss, R. A. Polym Eng Sci 1997, 37, 1936.
10. Kim, Y.; Kim, J. Colloid Polym Sci 2008, 286, 631.
11. Flitton, R.; Johal, J.; Maeda, S.; Armes, S. P. J Colloid Interface Sci 1995, 173, 135.
12. Shamsuri, A.; Daik, R.; Ahmad, I.; Jumali, M. J Polym Res 2009, 16, 381.
13. Ni, P.; Fu, S. In Colloidal Polymers Synthesis and Characterization; Elaissari, A., Ed.; Marcel Dekker: New York, 2003.
14. Sun, Y.; Ruckenstein, E. Synth Met 1995, 72, 261.
15. Omastova, M.; Kosina, S.; Pionteck, J.; Janke, A.; Pavlinec, J. Synth Met 1996, 81, 49.

16. Xie, H.-Q.; Liu, C.-M.; Guo, J.-S. Polym Int 1999, 48, 1099.
17. Bunsomsit, K.; Magaraphan, R.; O'Rear, E. A.; Grady, B. P. Colloid Polym Sci 2002, 280, 509.
18. Lascelles, S. F.; Armes, S. P. J Mater Chem 1997, 7, 1339.
19. Xiao-Jun, X.; Leong-Ming, G.; Kok-Siong, S.; Ming-Keong, W. J Appl Polym Sci 2004, 91, 1360.
20. Liu, J.; Wan, M. J Mater Chem 2001, 11, 404.
21. Omastova, M.; Trchova, M.; Kovarova, J.; Stejskal, J. Synth Met 2003, 138, 447.
22. Asaletha, R.; Bindu, P.; Indose, A.; Meera, A. P.; Valsaraj, S. V.; Weimin, Y.; Sabu, T. J Appl Polym Sci 2008, 108, 904.
23. Chuayjuljit, S.; Moolsin, S.; Potiyaraj, P. J Appl Polym Sci 2005, 95, 826.
24. Neoh, S. B.; Hashim, A. S. J Appl Polym Sci 2004, 93, 1660.
25. Asaletha, R.; Kumaran, M. G.; Thomas, S. Eur Polym J 1999, 35, 253.
26. Wei, M.; Lu, Y. Synth Metals 2009, 159, 1061.
27. Kim, D. K.; Oh, K. W.; Ahn, H. J.; Kim, S. H. J Appl Polym Sci 2008, 107, 3925.
28. Tassawuth, P.; Adisorn, C.; Nattaya, M.; Rathanawan, M. J Appl Polym Sci 2009, 112, 1552.
29. Jang, J.; Yoon, H. Adv Mater 2003, 15, 2088.
30. Shang, S.; Yang, X.; Tao, X.-M. Polymer 2009, 50, 2815.
31. Tang, M.; Wen, T.-Y.; Du, T.-B.; Chen, Y.-P. Eur Polym J 2003, 39, 151.
32. Pojanavaraphan, T.; Magaraphan, R. Polymer 2010, 51, 1111.